AD-A197 249

SEMI-ANNUAL REPORT: ONR CONTRACT

THE ANALYTICAL EXPONENTIAL DECAY COEFFICIENT OF THE SUBMARINE LIGHT FIELD

ONR Contract Number: NO0014-86-K-0606

Introduction

During the third semi-annual period of this contract the NORDA optical

model developed during my stay with Naval Ocean Research and Development

Activity, National Space Technology Laboratories, Bay St. Louis, MS was ported

to the Vax 8700 facility at the University of North Carolina/Greensboro. The

model was used to extend the work accomplished earlier on the Kw coefficient to

demonstrate the serious systematic errors in assuming this coefficient to be a

constant and this was reported at the Ocean Sciences 88 joint AGU/ASLO meetings

in New Orleans, LA.   The NORDA optical model was then used to simulate the

effects of water Raman emission on the submarine light field and the optical

properties derived from the irradiance measurements of this field.   The initial

modeling efforts were for the light field at 520 nm in clear ocean water and

the results were confirmed by the data from the Biowatt-NORDA cruise in the

Sargasso Sea, August 1987, using the NORDA-developed POSSY (Particle- Optical

Sampling System) instrument.   The following manuscript, coauthored with Dr.

Alan D. Weidemann of NORDA, detailing these results was submitted to the

journal Applied Optic

DTIC
S ELECTE D
JUN 1 7 1988
C₉
D

88   6   2   015

OPTICAL MODELING OF CLEAR OCEAN LIGHT FIELDS:
RAMAN SCATTERING EFFECTS

Robert Hans Stavn
University of North Carolina/Greensboro
Department of Biology
Greensboro, NC 27412

Alan Dean Weidemann
Naval Ocean Research and Development Activity
Code 331
National Space Technology Laboratories, MS 39529

Accesion For		
NTIS CRA&I		☑
DTIC TAB		☐
Unannounced		☐
Justification		
By *per ltr*		
Distribution /		
Availability Codes		
Dist	Avail and/or Special	
A-1		

DTIC
COPY
INSPECTED
4

88   6   2   015

ABSTRACT

A Monte Carlo simulation (the NORDA optical model) and the Three-Parameter Model of the submarine light field are used to analyze the effect of water Raman emission at 520nm in clear ocean waters. Reported optical anomalies for clear ocean waters at longer wavelengths (520nm +) are explained by the effects of water Raman emission and the simulation results are confirmed by Biowatt-NORDA observations made in the Sargasso Sea. A new optical parameterization for clear ocean water is proposed.

2.

I. INTRODUCTION

Recent reports of anomalous optical properties for clear ocean waters are casting doubts on the adequacy of current paradigms for the optical properties of clear ocean water. These anomalous optical properties are calculated from standard irradiance measurements. Specifically, Prieur and Sathyendranath[1] and Spitzer and Wernand[2] report that certain values of calculated absorption coefficients for clear ocean water in the 500nm - 600nm wavelength region are less than the currently accepted values for the absorption coefficient of molecular water. Since clear ocean water is more than molecular water and has admixtures of other materials, this result is clearly a problem.

In addition to the relatively few calculations of the absorption coefficient, there are for the 500nm - 600nm wavelength region many reports of the downwelling exponential decay coefficient (diffuse attenuation coefficient) K_d being of the same order of magnitude as or less in magnitude than K_w, an exponential decay coefficient postulated for molecular water.[3,4,5,6] The coefficient K_w is not a constant like the absorption coefficient for molecular water,[1,7] but one interpretation is that it represents the minimum possible exponential decay coefficient that could exist for molecular water. Thus calculated exponential decay coefficients that are

3.

less than those postulated for molecular water are clearly also a problem. The overall pattern noted by Siegel and Dickey[5] in this region is a decrease in the K_d coefficient with depth as the wavelength increases. Sugihara et al[8] have also noted a decrease in the exponential decay coefficient of the upwelling irradiance, K_u, with depth.

The patterns noted for the K_d coefficient have also been reported for the wavelength region of 600nm - 700nm by the authors noted above, while Morel and Prieur[9] were among the first to note a precipitous drop in the K_u coefficient for clear ocean waters at 685nm. Their explanation of this anomalous optical property was fluorescent emission by chlorophyll a and it is widely accepted.[10] The general decrease of K_d with depth at other wavelengths cannot be explained by fluorescent emission at a few discrete wavelengths.[5,11]

The ability to analyze the clear oceans optically for concentrations of biological and minerogenic material and to determine optical energy budgets for biology, meteorology, and climatology depends on a reliable optical model of ocean waters that accounts for all significant physical-optical phenomena. Greater attention is being paid to the physical forcing of biological phenomena in clear oceans and the reciprocal feedback of growth of biological material on the physical forcings within the system.[12] Interpretation of satellite data depends on

reliable and robust optical models and parameters for the open ocean. Thus the inability to calculate reliable optical coefficients from measurements of irradiance in the longwave (520nm +) region of the optical spectrum may constitute a "crisis" in the current state of optical oceanography.

The obvious source of non-instrumental error in the calculated optical coefficients is internal light sources that violate the conservation of photon flux at a given wavelength and thus invalidate the standard optical calculations, which require this condition. Sugihara et al[8] explained the decrease with depth of the K_u parameter by water Raman emission in the mid-range wavelengths (500nm - 600nm) which exhibit very few or no obvious sources of fluorescence compared to the case at 685nm. Direct experimental evidence of the significance of water Raman emission in both clear ocean and coastal waters is provided by the extensive studies of Hoge and Swift[13,14] and Bristow et al[15] who use the Raman emission signal from an airborne laser to correct for laser stimulated fluorescence signals from chlorophyll a in the surface layers. The variations in the water Raman signal correct the variations in the fluorescence signal due to changes in the transparency of the surface layers. Exton et al[16] demonstrated a significant water Raman return from a laser stimulated laboratory water tank of 19 l capacity filled with natural seawater samples. These observations demonstrated a

5.

significant return from the OH stretch mode of water Raman

emission and there was even the possibility of a significant

return from the bending mode of the water molecule.

Since the purported effects of internal emission of radiant

flux include interactions with absorption and single- and

multiple-scattering processes, it has been difficult to

demonstrate unequivocally the possible effects of water Raman

emission with the simple quasi-single-scattering models that have

been attempted heretofore. The best accepted mathematical

description of the processes affecting the submarine light field

is the radiative transfer equation[17,18] which has no simple

analytical solution but does have the capability of dealing with

multiple-scattering. Rather than solving the radiative transfer

equation the normal procedure for dealing with it is to

approximate a solution with the Monte Carlo simulation method.

Poole and Esaias[19] have used their SALMON version Monte Carlo

model to study the effects of water Raman emission on a laser

stimulated radiance field. A Monte Carlo simulation of a solar

stimulated radiance-irradiance field has not yet been attempted.

The purpose of this paper is to utilize a Monte Carlo

simulation of the radiative transfer equation (the NORDA optical

model) to demonstrate the quantitative significance of water

Raman emission in clear ocean light fields. We will account for

all accepted optical processes in deep clear ocean waters and

6.

report on the data collected from a joint Biowatt-NORDA cruise in the Sargasso Sea that confirm the predictions of the model. A simple exact solution of the integrated version of the radiative transfer equation,[17] permitted by the Three-Parameter Model,[20] will be used to analyze the Monte Carlo output and translate the simulation results to practical field measurements. The optical calculations possible with the Three-Parameter Model allow a sensitive and robust analysis of water Raman emission effects with standard irradiance measurements. We will lay the basis for a new clear ocean optical parameterization that provides the baseline for all optical models of oceanic light fields.

II. NORDA OPTICAL MODEL and INPUT PARAMETERS

Monte Carlo modeling of submarine light fields is exemplified in the work of Kirk,[21] Plass and Kattawar,[22] and Gordon, Brown, and Jacobs,[23] all of which inspired the development of the NORDA optical model. In this model the light field is unpolarized and the optical coefficients are defined accordingly. Two of the optical coefficients are chosen in accordance with Morel's[24] Blue Water Model in the range of types T_3 - T_4. The Morel Blue Water Model is an optical parameterization of clear ocean water in which absorption is due only to molecular water, elastic scattering from the water molecule occurs due to fluctuation theory,[25] and large particle elastic scattering occurs from non-absorbing finely divided quartz-like matter.[26] We use the

7.

conventional Monte Carlo technique where the interactions of a photon with the medium (absorption, elastic scattering, inelastic scattering) are determined from a random number and the appropriate optical coefficients. If the interaction is an absorption event the photon is terminated and a new photon enters the medium. If the interaction is an elastic scattering event a new random number determines whether the interaction is with a water molecule or a suspended, non-absorbing, quartz-like particle. After this determination is made another random number chooses the new trajectory of the photon from either the Rayleigh-type scattering geometry,[25,27] or the Petzold scattering geometry.[21,28] The additional optical coefficient featured in the NORDA optical model is the inelastic Raman scattering coefficient for the water molecule which is also chosen by a random number. If the interaction of the photon with the water molecule is an inelastic scattering event the photon is converted to one of longer wavelength determined by the mean frequency shift of $3357 cm^{-1}$ reported by Sugihara et al.[8] The new trajectory at the longer wavelength is determined by another random number from the Rayleigh-type scattering geometry which governs water Raman emission.[29] The photon at the longer wavelength then undergoes the absorption and elastic scattering events with the proper optical coefficients for the longer wavelength. We assume that no further higher order interactions occur at the longer

8.

wavelength.

The mean frequency shift of $3357cm^{-1}$ represents the two
fundamental OH stretch vibration modes of the water molecule that
are further modified by hydrogen bonding and rotational fine
structure.[29,30,31,32] These interactions cause a broadband of
emissions around the mean frequency shift so that water Raman
emissions occur over an optical band[8] of about 30nm-50nm rather
than occurring as a line emission as has been assumed in some
models.

The broad band of water Raman emission means that for any wave
length we choose to study there will be water Raman emissions
contributed from various source wavelengths. We are able to
account for this conveniently in the model because of the nature
of radiant energy measurements made by modern solid-state optical
detectors. These detectors actually measure an optical band and
not a line; routinely we can measure a nominal central wavelength
$\pm$ 5nm. Thus we measure radiant energy or photon flux over a 10nm
band width and the optical coefficients calculated from these
measurements are averages over the measured band; the most
probable wavelength associated with this average is the nominal
or central wavelength. The water Raman emission from a nominal
source wavelength in the model is then the averaged emission over
a 10nm bandwith, and the average water Raman emission function is
determined from the nominal wavelength of the source photons. If

9.

we are able to determine the source photons over a bandwidth of 10nm, then we are able to determine the emitted photons over a bandwidth of 10nm. This fact must be taken into account when determining the portion of the water Raman emission that can be detected in the model which simulates the conditions of measurement that occur with actual solid-state optical sensors.

Published Raman scattering cross-sections, from which inelastic Raman scattering coefficients can be calculated, are integrated over different limits of frequency shifts. We corrected for this by taking Sugihara's data and planimetrically integrating it over a very broad frequency shift band. We then determined the emission over specified frequency shift bands and brought various published coefficients into direct comparison. This also allowed the determination of water Raman emission over particular frequency shift bands of interest that were related to particular optical wavebands of interest. Since the most complete data set from the Biowatt-NORDA cruise was taken at 520 $\pm$ 5nm, the water Raman emission for this study was generated in that waveband at that central wavelength. We determined the energy emitted in this optical waveband by the water Raman emission function centered at a frequency shift of 3357cm^{-1} which yields a source wavelength of 442.7nm. The water Raman emission in the 520 $\pm$ 5nm waveband generated from the 442.7nm source wavelength amounted to about 51% of the total emitted from that

10.

source wavelength. We were able to generate about 95% of the possible water Raman emission at 520 ± 5nm by considering the emission function for the 10nm waveband above the 442.7 ± 5nm waveband (452.7 ± 5nm) and the 10nm waveband below the primary emission source (432.7 ± 5nm). The water Raman emission from the 432.7nm source was centered at 506.2nm and about 11% of this emission occurred in the 520 ± 5nm waveband. The water Raman emission from the 452.7nm source was centered at 533.8nm and about 8% of this emission occurred in the 520 ± 5nm waveband. These percentiles were used to calculate Raman scattering coefficients for photons in the 10nm wavebands centered at 432.7nm, 442.7nm, and 452.7nm and emitted at 520 ± 5nm. The estimate of the water Raman emission for clear ocean water at 520 ± 5nm was the sum of the photons generated at the three source wavebands.

We investigated three published Raman scattering cross-sections for molecular water: Chang and Young,[33] Sugihara et al,[8] and Slusher and Derr.[34] For the wavelengths investigated the Chang and Young cross-section was the smallest and the Slusher and Derr cross-section was the largest. The two cross-sections differed by a factor of five. The Sugihara et al cross-section was always intermediate in value between the other two. For these simulations the Chang and Young cross-section was used for a "low estimate" of the Raman scattering coefficient and the Slusher and

11.

Derr cross-section was used for a "high estimate" of the Raman scattering coefficient. The Raman coefficient for a given wavelength was determined by the λ^{-4} relationship and the geometry of the emission was taken as a Rayleigh scattering geometry.[29,35]

It was necessary to establish the conditions external to the model ocean. Skylight was not included to simplify the calculations and the solar beam entered the model ocean at an angle of 11° from the zenith. This solar zenith angle was chosen to minimize the effects of simplistic relationships between optical properties that can occur due to the extreme symmetry of the light field under conditions of zenith sun. One of the major comparisons in this paper is between photons penetrating the model ocean from the solar beam and photons generated by Raman scattering of shorter wavelength solar photons from the water molecules. The photon fluxes from the solar beam penetrating the model ocean at 432.7 ± 5nm, 442.7 ± 5nm, 452.7 ± 5nm, and 520 ± 5nm were estimated from the optical air mass 1 model.[36]

A primary concern for investigations of ocean optical properties is whether a given optical property is of quantitative significance for oceanic light fields. Hoge and Swift have demonstrated that Raman emission is equal to or greater than fluorescence in terms of the return from a laser stimulated clear ocean system. Table 1 and Poole and Esaias[19] indicate that the

12.

Raman scattering coefficient is of the same order of magnitude as the Rayleigh-type elastic scattering coefficient from water molecules due to fluctuation theory. Because of the concern to demonstrate quantitative significance of water Raman scattering for clear ocean light fields, the assumptions of the NORDA optical model have been made as conservative as possible. First, although we have eliminated skylight from the model to make the calculations simpler, this has also removed a potential source of water Raman emission since the skylight represents short wavelength photons removed from the solar beam. Second, the Raman scattering cross-sections used to determine the Raman scattering coefficients were determined for distilled water. The dissolved chloride in seawater would increase the Raman scattering cross-section[35] by about 10%. Third, the Raman scattering cross-sections used in this study were determined from room temperature observations (25° C) for which the Raman scattering cross-section is about 10% less [35,37] than would be the case at 0° C. This means that the water Raman emission for the deeper cooler layers is underestimated in this model which is held uniform thermally. The NORDA simulation therefore represents a "tropical ocean, uniform in thermal profile, composed of seawater and non-absorbing finely divided quartz, and undergoing the Raman emission of unmodified molecular water". This formulation yields the minimal amount of expected Raman emission.

The model was implemented as follows. The air/water interface was flat and the model ocean was infinitely deep optically. At the chosen water Raman emission wavelength (520 $\pm$ 5nm) five runs of 10^6 solar photons each were made with a mean and standard error of the mean determined. Counters for the number of photons in the downwelling and upwelling vectorial irradiances and in the downwelling and upwelling scalar irradiances were set at 5 meter intervals. The solar photon fluxes at the shorter wavelengths chosen to be the photon sources for the water Raman emission were adjusted relative to the solar photon flux at 520 $\pm$ 5nm and five model runs were made at each source wavelength. A separate set of counters for the water Raman emission photons was established at 5 meter intervals and the same irradiances established for the Raman photons as for the solar photons at 520 $\pm$ 5nm. This information was used to determine the downwelling vector irradiance and the scalar irradiance for the Three-Parameter Model.[20] Calculations of the average cosine of the submarine light field were made for the solar photons alone, the Raman photons alone, and the combined photon flux as it would be measured by an actual light sensor. The absorption coefficient was calculated from the combined photon flux and compared with the absorption coefficient for molecular water, determined from the tables of Smith and Baker.[38] These calculated parameters proved to be sensitive indicators of the effects of water Raman

14.

emission and they can be calculated from standard irradiance measurements made at sea.

III. NORDA OPTICAL OBSERVATIONS

Optical measurements were collected during August, 1987 at 13 stations in the western Sargasso Sea at about 34° N and 70° W. Irradiance measurements were made with a Biospherical Instruments model 1048 Mer spectroradiometer. This permitted measurement of downwelling irradiance at 13 wavelengths (10nm bandwidth at 50% of peak), upwelling irradiance at 8 wavelengths, and downwelling and upwelling scalar irradiances at 4 wavelengths. Due to the loss of one of the downwelling scalar sensors on the first cast, the average cosine (requiring the vector and scalar irradiance data) could only be calculated for 3 wavelengths: 441nm, 488nm, and 520nm. Additional instrumentation on the optical package included a 25cm transmissometer operating at 660nm (Sea Tech), temperature and conductivity sensors (Sea Bird), 2 axis tilt and roll sensors, and a fluorometer/nephelometer (in fluorometer mode, Sea Mar Tech). The fluorometer operated at a broadband excitation (120nm bandwidth) with peak excitation at 450nm (Corning filters 4-72 and 5-60); emission was measured with a sharp high pass filter at 640nm (Corning 2-64). This optical suite was attached to an Ocean Dynamics Rosette (20 8-liter Niskin bottles) for collection of water samples. The complete package is termed the POSSY (Particle Optical Sampling System).

IV. RESULTS

The nature of the radiant fluxes at 520 $\pm$ 5nm simulated by the
NORDA optical model for a clear ocean is indicated in
Figs. 1 - 6. The downwelling irradiances due to the solar photon
flux and to water Raman emission are equivalent at about 115m for
the high estimate simulation (Fig. 1) and at about 160m for the
low estimate simulation (Fig. 2). Summing the two fluxes
indicates that the total irradiance measured by an ambient light
sensor is due more and more to water Raman emission with an
increase in depth until the water Raman flux becomes orders of
magnitude greater than the solar flux. The scalar irradiances
due to solar and water Raman photons become equivalent at about
85m for the high estimate simulation (Fig. 3) and at about 135m
for the low estimate simulation (Fig. 4).Beyond these depths the
total photon flux is predominantly water Raman emission. The
upwelling irradiances due to solar and water Raman photons become
equivalent at only 10m depth for the high estimate simulation
(Fig. 5) and at 55m depth for the low estimate simulation
(Fig. 6). Again at greater depths the total photon flux is
predominantly water Raman emission.

Optical parameters calculated from the solar photon flux and
the water Raman emission flux are plotted in Fig. 7: a comparison
of the average cosines for water Raman photons alone, for solar
photons alone, and for the total photon flux. The variation due

16.

to high and low estimate simulations is also indicated. The
average cosine of water Raman photons in the first 15m or so of
the surface layer is negative (-0.15 at the surface), indicating
a net upward flow of photons. At greater depths the average
cosine increases to about 0.1 indicating that the integrated flow
of water Raman photons is nearly isotropic. By contrast, the
average cosine of the solar photons is as high as 0.92 at the
surface and decreases slightly to 0.85 at 100m depth, indicating
a distinctly downward directional trend for the solar photon
flux. The average cosine plot for the total photons is dominated
by solar photons in the surface layers and becomes dominated by
water Raman photons below about 80m.

The absorption coefficients calculated from the total photon
flux by the Three-Parameter Model[20] are plotted in Fig. 8 along
with the absorption coefficient for seawater used in the NORDA
model simulation. The calculated absorption coefficients are
always less than the actual absorption coefficient used in the
simulation. The calculation of the absorption coefficient from
the solar photon flux alone reproduces the absorption coefficient
used in the simulation. The low estimate water Raman simulation
produces an absorption coefficient that just differs from the
actual absorption coefficient near the surface while the high
estimate water Raman simulation produces an absorption
coefficient that differs significantly from the actual absorption

17.

coefficient even just below the air/water interface. With increasing depth the deviation of the calculated absorption coefficient from the actual absorption ccefficient increases markedly.

Average cosines determined from the NORDA optical data and the Monte Carlo simulation results at 520 $\pm$ 5nm are compared in Fig. 9. This is a plot of raw data with no signal processing. The average cosines from the Biowatt-NORDA cruise were calculated from irradiance measurements in the Sargasso Sea, 33° 40.8' N, 69° 53.44' W, taken from the R/V Endeavor near the Biowatt mooring. The average cosines for solar photons alone and for total photons from the NORDA simulation differ markedly as was noted before, and the average cosines from the Sargasso Sea data are bracketed by the average cosines of the simulated total photon flux.

V. DISCUSSION

We initially described a possible "crisis" in optical oceanography where the irradiance measurements that have been made in clear ocean waters by many investigators yield calculated optical coefficients that are anomalous, i.e. absorption coefficients and exponential decay coefficients smaller in magnitude that those ascribed to molecular water. These anomalies are usually explained as "instrumental problems" with either the measurement of low light levels or light leakage from the shorter

18.

wave portion of the electromagnetic spectrum to the longer wave light sensors; the anaomalies occur at wavelengths of 520nm up to the "red limit" of the visible spectrum. In the region of 550nm or less the possibility of significant light leakage has apparently been ruled out (C.R. Booth, Biospherical Instruments, Inc. personal communication). For t.ie wavelength investigated in this study we can also rule out instrumental sensitivity as the source of the anomalies because the postulated effects of the water Raman emission show up before the typical instrumental sensitivity limits are reached (Fig. 9), with the effects being demonstrable even at the air/water interface. Certain discrete wavelengths, e.g. 685nm, are known to be regions of fluorescent emission from materials such as chlorophyll a and as such the optical anomalies at 685nm can be explained. Siegel and Dickey[5] point out that the generalized decrease in exponential decay coefficients with depth occurs at many wavelengths where there are no known fluorescence sources.

Water Raman scattering occurs continuously over the entire optical spectrum with the same wavelength dependence as elastic Rayleigh scattering and fluctuation theory scattering. Figures 1 - 6 demonstrate how water Raman scattering can account for the anomalous results of optical calculations from the longer wavelength irradiances in clear ocean water where there are no known fluorescence sources. The solar photons at 520 ± 5nm are

19.

absorbed relatively quickly due to the absorption coefficient of molecular water being much increased at longer wavelengths. The water Raman emission from more deeply penetrating photons at shorter wavelengths becomes more important with depth until in the region of about 100m depth the light field is composed of about half penetrating solar photons of $520 \pm 5nm$ wavelength and half water Raman emission photons at $520 \pm 5nm$ wavelength. At greater depths the light field is transformed to one due almost entirely to water Raman emission. Clearly, the optical coefficients calculated from such a non-conservative light field will be corrupted.

Since the optical coefficients calculated from light fields affected by internal emission are unreliable and not indicative of the conservative light fields they were designed for, what would be the best coefficients to work with in such light fields, i.e. which of the reasonably obtainable measurements and coefficients would give the most information? We can eliminate the empirical exponential decay coefficients (diffuse attenuation coefficients) such as K_d and K_u for the simple reason that although conveniently measured and calculated, they are composite coefficients that are the product of at least 3 separate and identifiable optical coefficients. Thus variations [7,39] in the "k coefficients" are difficult enough to interpret in a conservative light field let alone a non-conservative one.[7] The

coefficients that can be calculated from the irradiance measurements used for the Three-Parameter Model (downwelling irradiance, upwelling irradiance, and scalar irradiance) show promise of giving useful information from light fields affected by internal emission. They are not composite coefficients and reliable inferences from them are possible. Consider the properties of the average cosine and the absorption coefficient calculated from the Three-Parameter Model.

The average cosine of the Three-Parameter Model is the inverse of the mean path traveled by photons per meter.[20,40] It varies from 0.0 - 1.0 with a small value indicating a highly diffused nearly isotropic light field where the photons are travelling nearly uniformly in all directions; while a large value of the coefficient indicates a highly directional light field with the photon path biased, for the coordinates used in oceanography, in a strongly downward direction. Negative values for the same coordinates indicate a net flow upward. A small value of the average cosine is expected from a light field that is dominated by a nearly uniform source of photons while a large value of the average cosine is expected for a light field with a highly directional photon source, such as the solar beam. The general pattern of variation of the average cosine in natural waters is that of a high value near the surface and a gradual decrease with depth as the photons are increasingly diffused by single- and

21.

multiple-scattering. The minimum possible value of the average

cosine in a clear ocean with a solar photon source is 0.53 at

400nm as predicted by Plass et al[41] and this value has been

confirmed in simulations with the NORDA optical model. The

minimum possible value of the average cosine with a solar photon

source increases for longer wavelengths. The variation in the

average cosine for solar photons at 520 $\pm$ 5nm is 0.92 at the

surface to 0.85 at 100m (Fig. 7) as determined from the NORDA

Monte Carlo simulation. This strongly directional nature of the

solar photon field at this wavelength is to be expected when we

see that absorption dominates over scattering at this wavelength

(Table 1). When the water Raman photons are added to the solar

photons in the simulation the average cosine at 100m drops to

0.47 - 0.65 and a light field results that is more diffuse than

can be accounted for by absorption and scattering of solar

photons in clear ocean waters. Thus the NORDA data from the

Sargasso Sea with an average cosine in the range of 0.5 - 0.6 at

100m (Fig. 9) indicate that the light field at that depth cannot

be due to penetrating solar photons alone. Spitzer and Wernand[2]

report an anomalously low average cosine of 0.73 for 520nm at 55m

depth in oligotrophic central Atlantic waters in agreement with

NORDA observations (Fig. 9) and within the band of possible

values predicted from the NORDA simulation. The average cosine

thus serves as a sensitive indicator of the nature of the light

22.

field in clear ocean waters.

The Sargasso Sea station for the NORDA data was clear ocean water with a fluorescing layer (fluorescence measured at 640nm - 690nm), presumably algal cells, at a depth of about 80 - 100m. This shows up as an interruption in the downward trend of the average cosine (Fig. 9) due to the absorption by the cells which decreases the mean photon path. The trend of the average cosine in the layers just above implies a greater decrease of the average cosine with depth if the fluorescing layer were not present. The NORDA data from the surface layer indicate average cosine values both less than and greater than the values in the NORDA Monte Carlo simulation. This result is due to the fact that the simulation had only a level surface while the field data show the effects of wave focusing and defocusing on the mean photon path of the light field at the air/water interface. In addition, there were ship motion effects near the surface in the unfiltered data of Fig. 9.

The lack of conservation of penetrating photons at $520 \pm 5nm$, i.e. more photons present than would be expected if water Raman emission were not occurring, causes the calculated absorption coefficient to be too small, smaller in fact in clear ocean waters than the accepted absorption coefficient for molecular water (Fig. 8). The effect is present even at the air/water interface. We feel that these results from the NORDA simulation

explain the difficulty in calculating absorption coefficients in clear ocean waters at longer wavelenths as reported in the literature.[1,2] As depth increases the calculated absorption coefficient becomes smaller as the submarine light field becomes dominated by water Raman emission. Consequently, the value of the calculated absorption coefficient is demonstrated as a quantitative measure of the contribution of the emitted photon flux to the measured submarine light field.

The analysis reported here for $520 \pm 5nm$ is being applied to other wavelengths. The trends that are evident at this relatively short wavelength extend to the longer wavelengths in the 500 - 600nm wavelength region. The next logical extension of these results is to investigate the effects of varying amounts of absorbing dissolved/suspended material that will absorb photons which might have otherwise interacted with the water molecule. The results of Hoge and Swift, Bristow et al, and Poole and Esaias demonstrate that the expected water Raman emission will vary depending on the nature of the other materials present in the ocean water. Even in coastal waters, however, Carder[42] has demonstrated a probable water Raman emission effect on the K_d coefficient at 625nm.

VI.SUMMARY

The NORDA simulations and data reported here constitute the
first comprehensive optical description of the clearest ocean
waters. Optical oceanography has traditionally used the optical
parameterization of the clearest possible ocean waters as the
baseline for the description and modeling of all oceanic light
fields.[9,17,38] These Blue Water type models are represented as
containing the fundamental optical parameters needed to describe
the optical and radiative flux events of the clearest ocean
waters. Only the additive combination of the clear ocean optical
parameters with the optical parameters of any material added in
solution or suspension is required to predict the optical
environment of the ensuing ocean model: transparency,
backscattered flux recorded by satellites, meteorological and
biological energy budgets, etc. We propose that the fundamental
optical parameterization of the clearest ocean waters to be used
for further ocean optical modeling contain: the absorption
coefficient for the water molecule, the elastic scattering
coefficient for the water molecule, the elastic scattering
coefficient for finely divided suspended quartz-like material,
and the inelastic Raman scattering coefficient for the water
molecule.

REFERENCES

1. L. Prieur and S. Sathyendranath, "An Optical Classification of Coastal and Oceanic Waters Based on the Specific Spectral Absorption Curves of Phytoplankton Pigments, Dissolved Organic Matter, and Other Particulate Materials," Limnol. Oceanogr. 26, 671 (1981).

2. D. Spitzer and M. R. Wernand, "In Situ Measurements of Absorption Spectra in the Sea," Deep-Sea Res. 28A, 165 (1981).

3. I. P. DePalma and D. F. Reid, "Optical Measurements with Related Chemical, Biological, and Physical Parameters from the Central Equatorial Pacific Ocean," NORDA Tech. Note 337 (1986).

4. H. Pak, D. W. Menzies, and J. C. Kitchen, "Optical Dynamics Experiment (ODEX) Data Report R/V Acania Expedition of 10 Oct thru 17 Nov 1982. Vol. 6: Scalar Spectral-Radiometer Data," College of Oceanography, Oregon State University, Corvallis, Oregon, ONR Data Report 124, Ref 86-10, Sept. (1986).

5. D. A. Siegel and T. D. Dickey, "Observations of the Vertical Structure of the Diffuse Attenuation Spectrum," Deep-Sea Res. 34, 547 (1987).

6. B. J. Topliss, "Optical Measurements in the Sargasso Sea: Solar Stimulated Chlorophyll Fluorescence," Oceanol. Acta

8, 263 (1985).

7. R. H. Stavn, "Lambert-Beer Law in Ocean Waters: Optical Properties of Water and of Dissolved/Suspended Material, Optical Energy Budgets," Appl. Opt. 27, 222 (1988).

8. S. Sugihara, M. Kishino, and M. Okami, "Contribution of Raman Scattering to Upward Irradiance in the Sea," J. Oceanogr. Soc. Japan 40, 397 (1984).

9. A. Morel and L. Prieur, "Analysis of Variations in Ocean Color," Limnol. Oceanogr. 22, 709 (1977).

10. H. R. Gordon, "Diffuse Reflectance of the Ocean: the Theory of its Augmentation by Chlorophyll a Fluorescence at 685nm," Appl. Opt. 18, 1161 (1979).

11. D. A. Siegel, C. R. Booth, and T. D. Dickey, "Effects of Sensor Characteristics on the Inferred Vertical Structure of the Diffuse Attenuation Coefficient Spectrum," Proc. Soc. Photo-Opt. Instrum. Eng. 637, 115 (1986).

12. R. C. Dugdale, F.P. Wilkerson, R. T. Barber, D. Blasco, and T. T. Packard, "Changes in Nutrients, pH, Light Penetration and Heat Budget by Migrating Photosynthetic Organisms," Oceanol. Acta (in Press).

13. F. E. Hoge and R. N. Swift, "Airborne Simultaneous Spectroscopic Detection of Laser-Induced Water Raman Backscatter and Fluorescence from Chlorophyll a and Other Naturally Ocurring Pigments," Appl. Opt. 20, 3197 (1981).

28.

14. F. E. Hoge and R. N. Swift, "Airborne Detection of Oceanic Turbidity Cell Structure Using Depth-Resolved Laser-Induced Water Raman Backscatter," Appl. Opt. 22, 3778 (1983).

15. M. Bristow, D. Nielsen, D. Bundy and R. Furtek, "Use of Water Raman Emission to Correct Airborne Laser Fluorosensor Data for Effects of Water Optical Attenuation," Appl. Opt. 20, 2889 (1981).

16. R. J. Exton, W. M. Houghton, W. Esaias, R. C. Harriss, F. H. Farmer, and H. H. White, "Laboratory Analyis of Techniques for Remote Sensing of Estuarine Parameters Using Laser Excitation," Appl. Pot. 22, 54 (1983).

17. N. G. Jerlov, Marine Optics (Elsevier, Amsterdam, 1976).

18. R. W. Preisendorfer, Hydrologic Optics (U. S. Department of Commerce, NOAA-ERL, Washington, DC, 1976).

19. L. R. Poole and W. E. Esaias, "Water Raman Normalization of Airborne Laser Fluorosensor Measurements: a Computer Model Study," Appl. Opt. 21, 3756 (1982).

20. R. H. Stavn, "The Three-Parameter Model of the Submarine Light Field: Radiant Energy Absorption and Energy Trapping in Nepheloid Layers Recalculated," J. Geophys. Res. 92, 1934 (1987).

21. J. T. O. Kirk, "Monte Carlo Procedure for Simulating the Penetration of Light into Natural Waters," CSIRO Div Plant Ind. Tech. Pap. 36, 16p (1981).

22. G. N. Plass and G. W. Kattawar, "Monte Carlo Calculations of Radiative Transfer in the Earth's Atmosphere-Ocean System:I. Flux in the Atmosphere and Ocean," J. Phys. Oceanogr. 2, 139 (1972).

23. H. R. Gordon, O. B. Brown, and M. M. Jacobs, "Computed Relationships Between the Inherent and Apparent Optical Properties of a Flat Homogeneous Ocean," Appl. Opt. 14, 417 (1975).

24. A. Morel, "In-Water and Remote Measurements of Ocean Color," Boundary-Layer Meteorol. 18, 177 (1980).

25. A. Morel, "Optical Properties of Pure Water and Pure Sea Water," in Optical Aspects of Oceanography, N. G. Jerlov and E. Steemann Nielsen, Eds. (Academic, London, 1974),p.1.

26. G. Kullenberg, "Observed and Computed Scattering Functions," in Optical Aspects of Oceanography, N. G. Jerlov and E. Steemann Nielsen, Eds. (Academic, London, 1974), p. 25.

27. E. J. McCartney, Optics of the Atmosphere. Scattering by Molecules and Particles, (Wiley-Interscience, New York, 1976).

28. J. T. O. Kirk, Light and Photosynthesis in Aquatic Ecosystems, (Cambridge, London, 1983).

29. D. A. Long, Raman Spectroscopy (McGraw-Hill, New York, 1977).

30. D. Eisenberg and D. Crothers, Physical Chemistry (Cummings, Menlo Park, 1979).

31. D. Eisenberg and W. Kauzmann, The Structure and Properties of Water (Oxford, New York and Oxford, 1969).

32. E. B. Wilson, JR., J. C. Decius, and P. C. Cross, Molecular Vibrations. The Theory of Infrared and Raman Vibrational Spectra (Dover, New York, 1980).

33. C. H. Chang and L. A. Young, "Seawater Temperature Measurement from Raman Spectra," Research Note 960, N62269-73-C-0073, sponsored by Advanced Research Projects Agency, ARPA Order No. 2194 (January 1974).

34. R. B. Slusher and V. E. Derr, "Temperature Dependence and Cross Sections of Some Stokes and Anti-Stokes Raman Lines in Ice Ih," Appl. Opt. 14, 2116 (1975).

35. A. T. Young, "Rayleigh Scattering," Appl. Opt. 20, 533 (1981).

36. P. R. Gast, "Solar Electromagnetic Radiation. Sec. 16.1. Solar Irradiance," in Handbook of Geophysics and Space Environments, S. L. Valley, Ed. (Air Force Cambridge Research Laboratories, Bedford, MA 1965).

37. G. E. Walrafen, "Raman Spectral Studies of the Effects of Temperature on Water Structure," J. Chem. Phys. 47, 114 (1967).

38. R. C. Smith and K. S. Baker, "Optical Properties of the

clearest Natural Waters," Appl. Opt. 20, 177 (1981).

39. G. Schellenberger, "Die Form der Raumlichen
    Strahlungsverteilung in Gewassern," Acta Hydrophys. 14, 207
    (1969).

40. G. Schellenberger, "Uber Zusammenhange Zwischen Optischen
    Parametern von Gewassern," Acta Hydrophys. 10, 79
    (1965).

41. G. N. Plass, T. J. Humphreys, and G. W. Kattawar,
    "Ocean-Atmosphere Interface: Its Influence on Radiation,"
    Appl. Opt. 20, 917 (1981).

42. K. L. Carder, R. G. Steward, T. G. Peacock, P. R. Payne,
    and W. V. Peck, "Spectral Transmissometer and Radiometer
    (STAR): Preliminary Results," Eos 68, 1683 (1987).

Table 1. Optical Parameters used in Monte Carlo Simulation of Clear Ocean Light Field with Solar Stimulated Water Raman Emission

	Source Wavelengths, nm			Emission Wavelength, nm
	432.7 ± 5	442.7 ± 5	452.7 ± 5	520 ± 5
Number of Solar Photons per Simulation Run &	6.27×10^5	6.91×10^5	7.91×10^5	10^6
Absorption Coefficient Sea Water, m^{-1} @	0.0145	0.0145	0.0147	0.0477
Fluctuation Theory Scattering Coefficient Sea Water, m^{-1} #	0.00542	0.00491	0.00445	0.00242
Particle Scattering Coefficient, m^{-1} *	0.0426	0.0416	0.0407	0.0354
Raman Scattering Coefficient	0.00051	0.0021	0.00032	---
Molecular Water, m^{-1} **	0.000097	0.00040	0.000060	

% Gast (1965)   @ Smith and Baker (1981)   # Morel (1974)   * Kirk (1983)

** High Estimate: Slusher and Derr (1975)
   Low Estimate : Chang and Young (1974)

Figure Legends

Fig. 1. Downwelling Irradiance E_d at 520nm due to solar photons (—■—), water Raman photons (—■—), and total photons (———). High estimate of Raman scattering coefficient. Sources of water Raman emission: 432.7 nm, 442.7nm, 452.7nm.
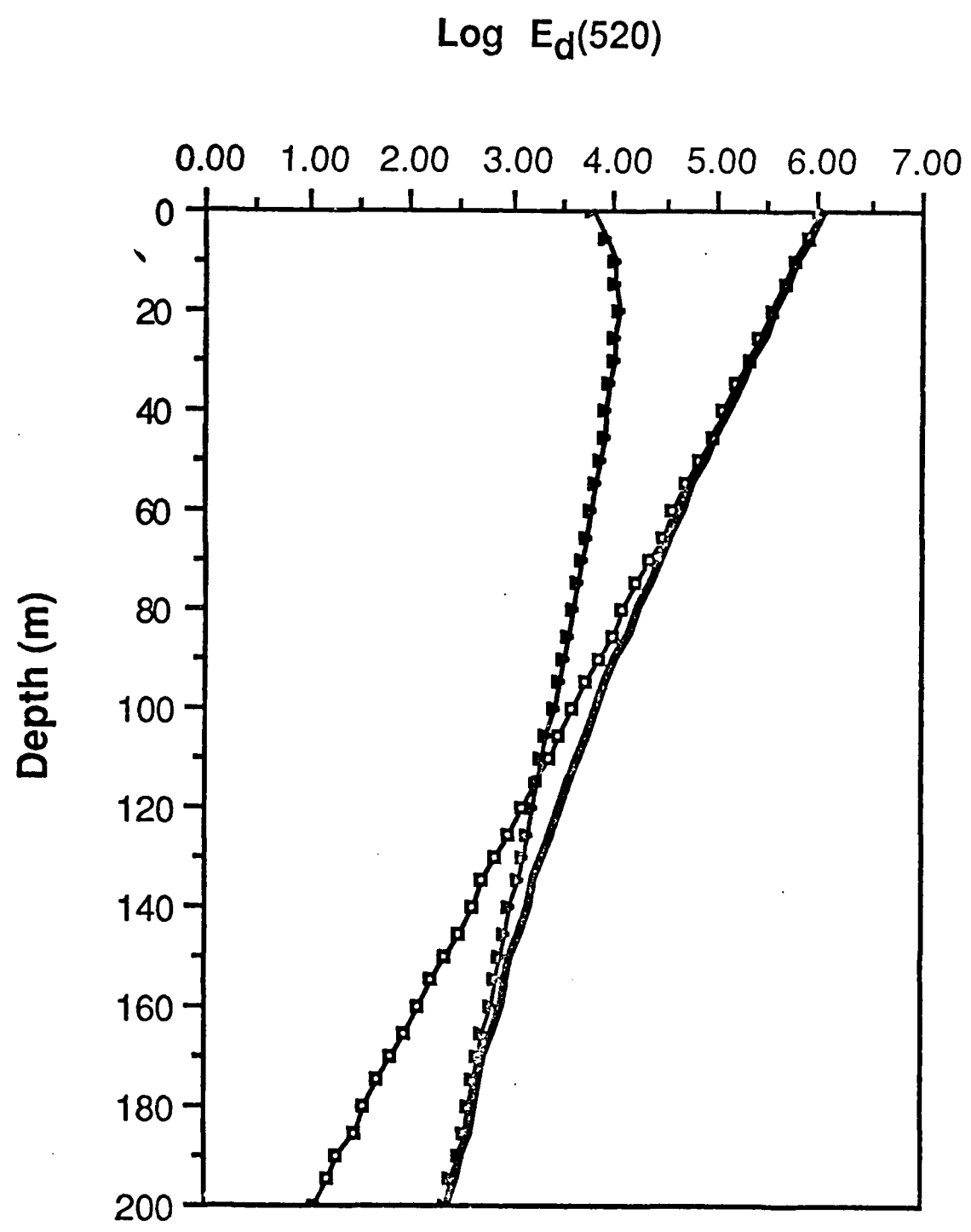
Fig. 2. Downwelling Irradiance E_d at 520nm due to solar photons (—■—), water Raman photons (—■—), and total photons (———). Low estimate of Raman scattering coefficient. Sources of water Raman emission: 432.7 nm, 442.7nm, 452.7nm.

Fig. 3. Scalar Irradiance E_o at 520nm due to solar photons (—■—), water Raman photons (—■—), and total photons (———). High estimate of Raman scattering coefficient. Sources of water Raman emission: 432.7nm, 442.7nm, 452.7nm.

Fig. 4. Scalar Irradiance E_o at 520nm due to solar photons (—■—), water Raman photons (—■—), and total photons (———). Low estimate of Raman scattering coefficient. Sources of water Raman emission: 432.7nm, 442.7nm, 452.7nm.

Fig. 5. Upwelling Irradiance E_u at 520nm due to solar photons (—■—), water Raman photons (—■—), and total photons (———). High estimate of Raman scattering

34.

coefficient. Sources of water Raman emission: 432.7nm, 442.7nm, 452.7nm.

Fig. 6. Upwelling Irradiance E_u at 520nm due to solar photons (——■——), water Raman photons (——•——), and total photons (———). Low estimate of Raman scattering coefficient. Sources of water Raman emission: 432.7nm, 442.7nm, 452.7nm.
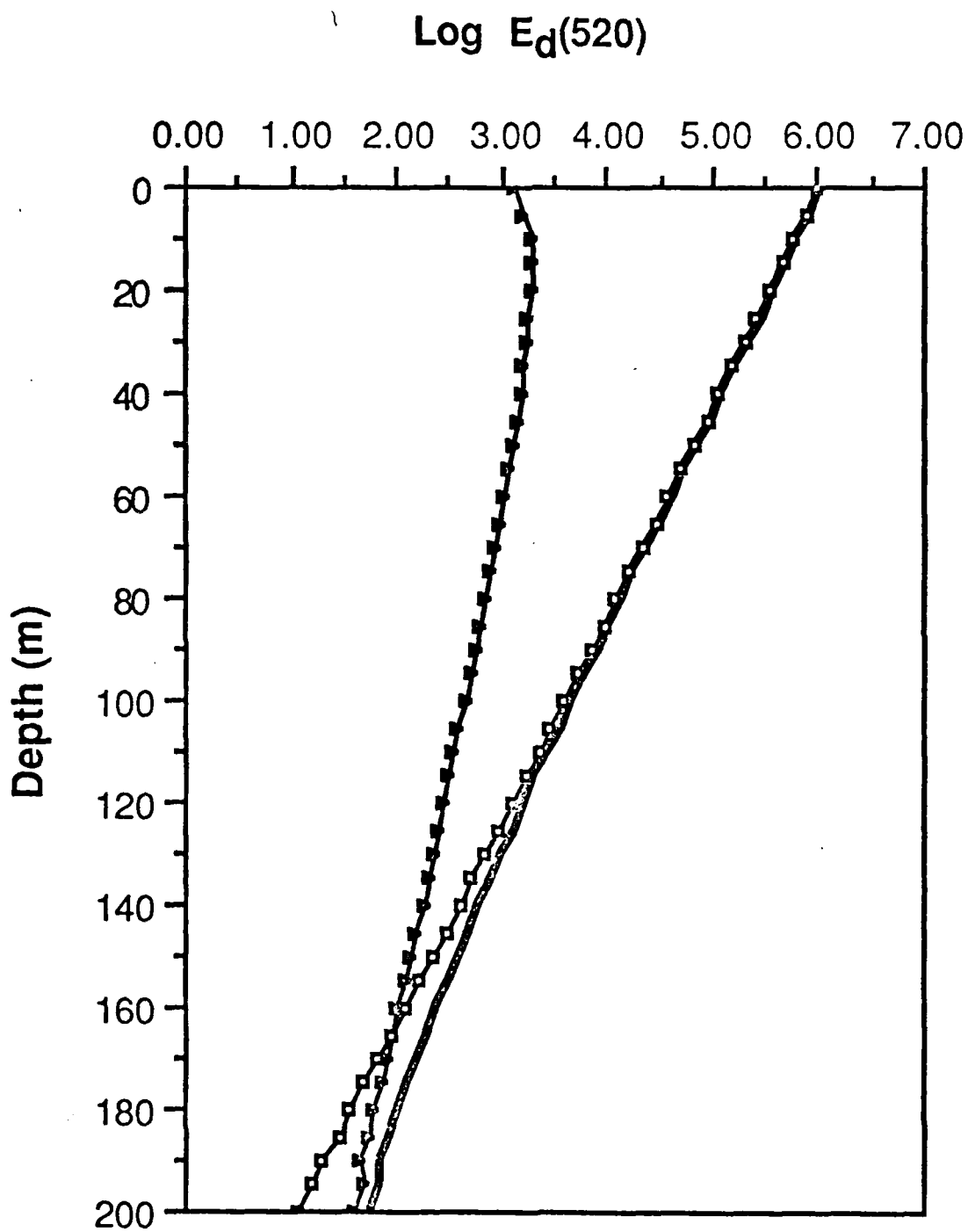
Fig. 7. Average cosine at 520nm of solar photons (——■——), Raman photons, high estimate Raman scattering coefficient (——■——), total photons high estimate Raman scattering coefficient (——◆——), total photons low estimate Raman scattering coefficient (——■——). Sources of water Raman emission: 432.7nm, 442.7nm, 452.7nm. Standard error of mean indicated in error bars.

Fig. 8. Absorption coefficient a(520) (——•——) calculated from total photon flux of high estimate Raman scattering coefficient, and a(520) coefficient (——•——) from total photon flux of low estimate Raman scattering coefficient. Standard error of mean indicated in error bars. Absorption coefficient aw(520) (———) for molecular water. Sources of water Raman emission: 432.7nm, 442.7nm, 452.7nm.
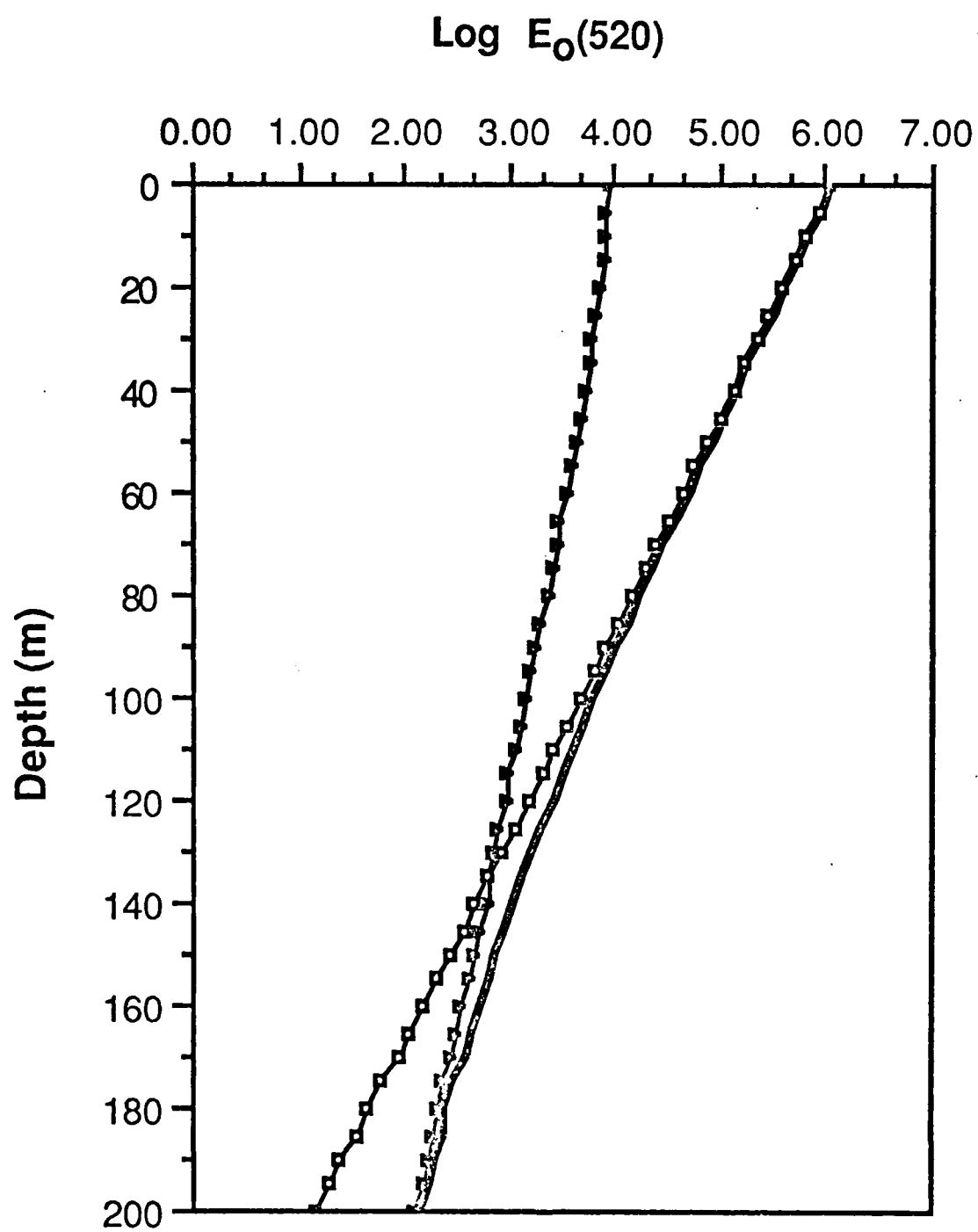
Fig. 9. Average cosine data at 520nm from Biowatt-NORDA cruise to Sargasso Sea. Average cosine for total photon flux

35.

of NORDA optical model with high estimate Raman
scattering coefficient (————). Average cosine for
total photon flux of NORDA optical model with low
estimate Raman scattering coefficient (——·——). Average
cosine for solar photon flux of NORDA optical model
(— — — —).

Log $E_d(520)$

Fig. 2

Log E$_d$(520)
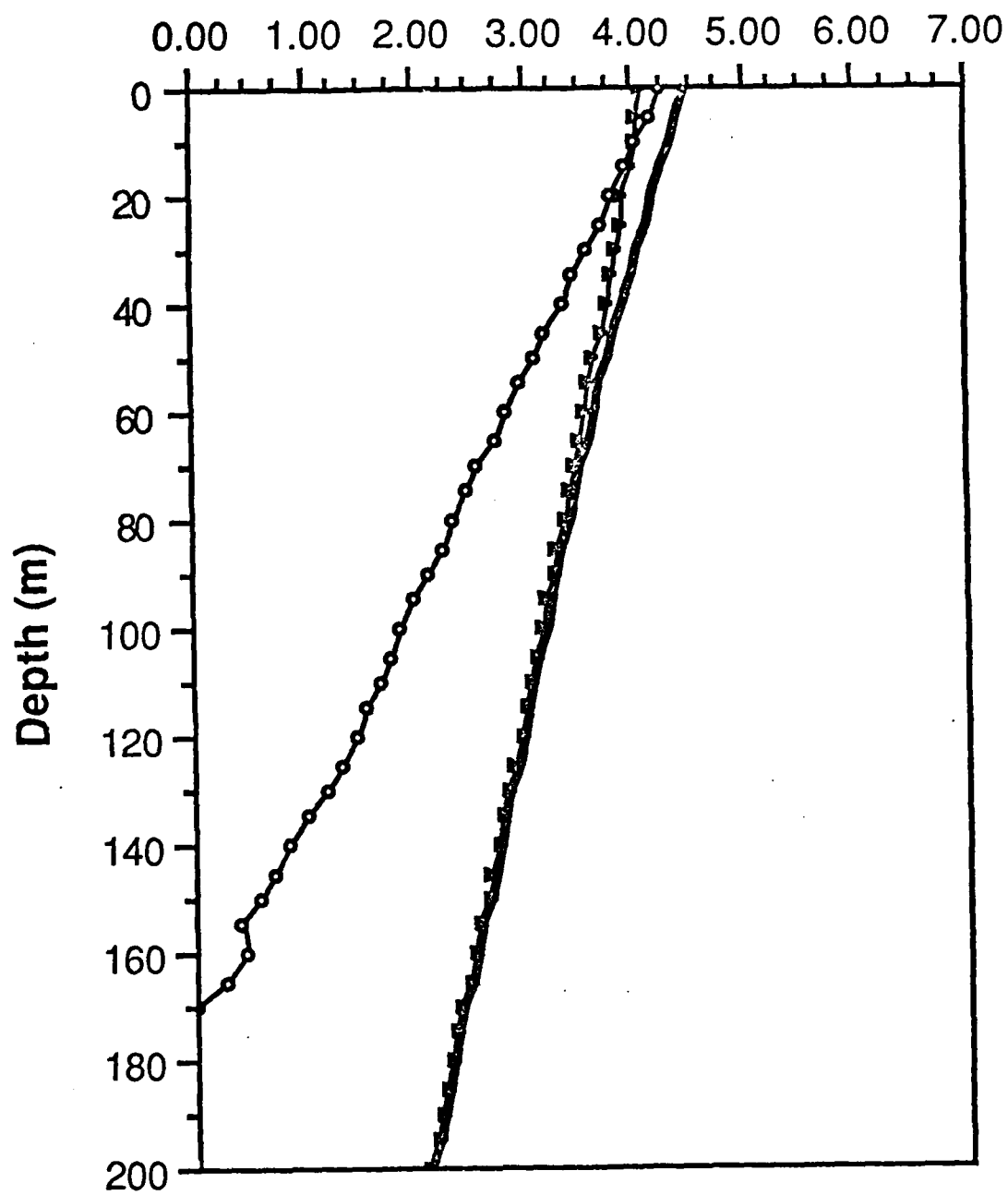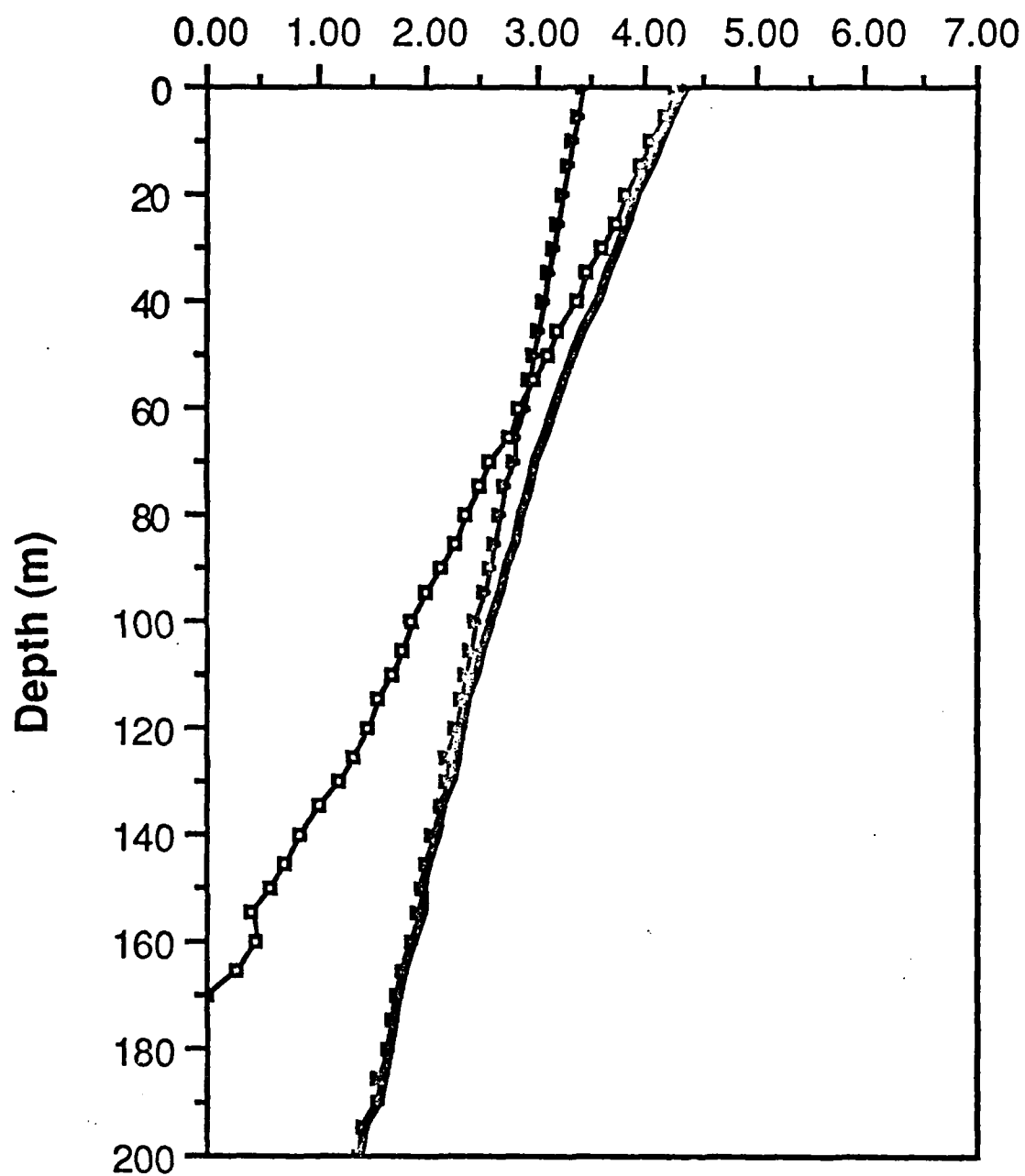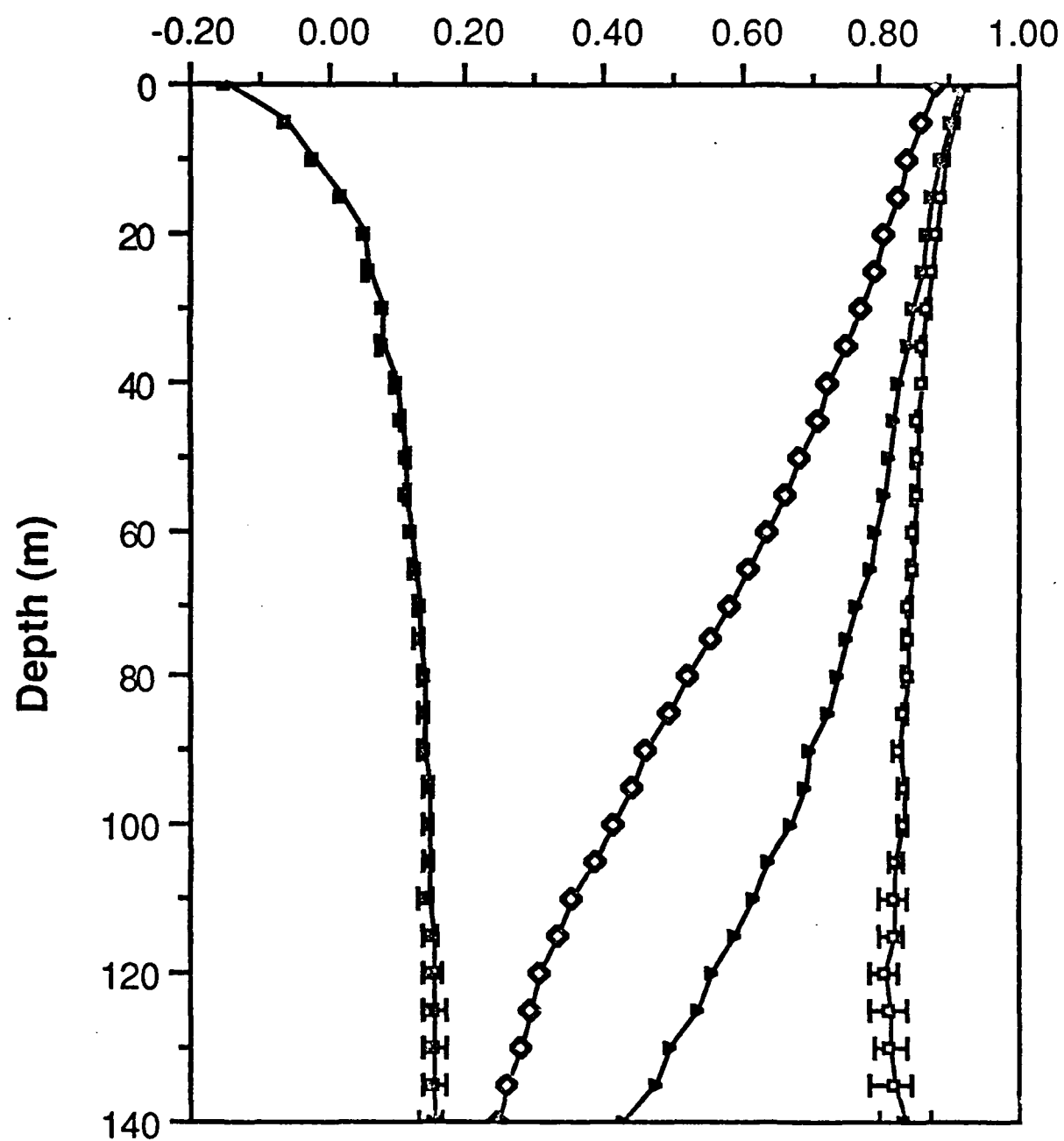
Log $E_O(520)$

Log $E_O(520)$

0.00 1.00 2.00 3.00 4.00 5.00 6.00 7.00
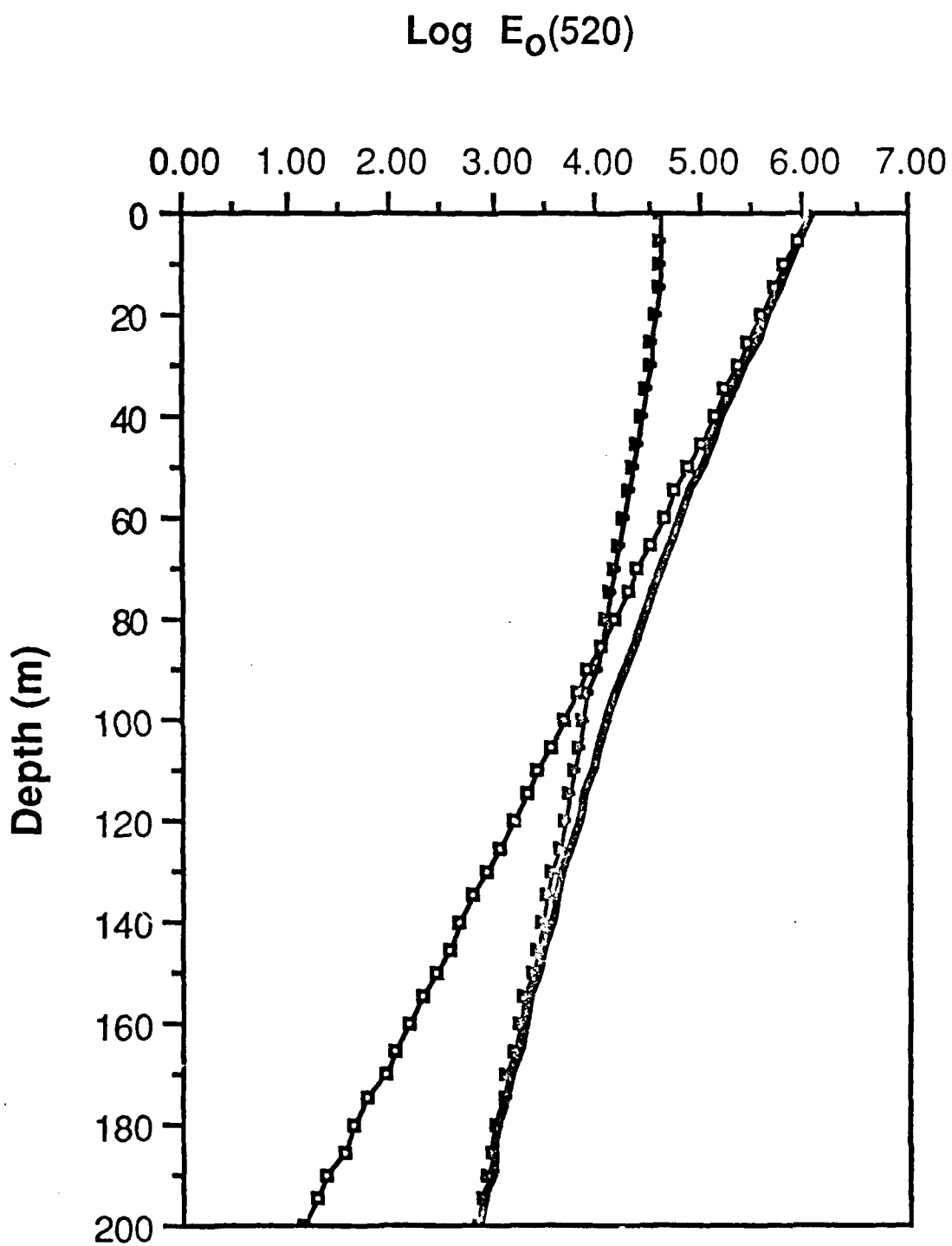
Log $E_u(520)$

Log $E_u(520)$

Average Cosine @ 520 nm
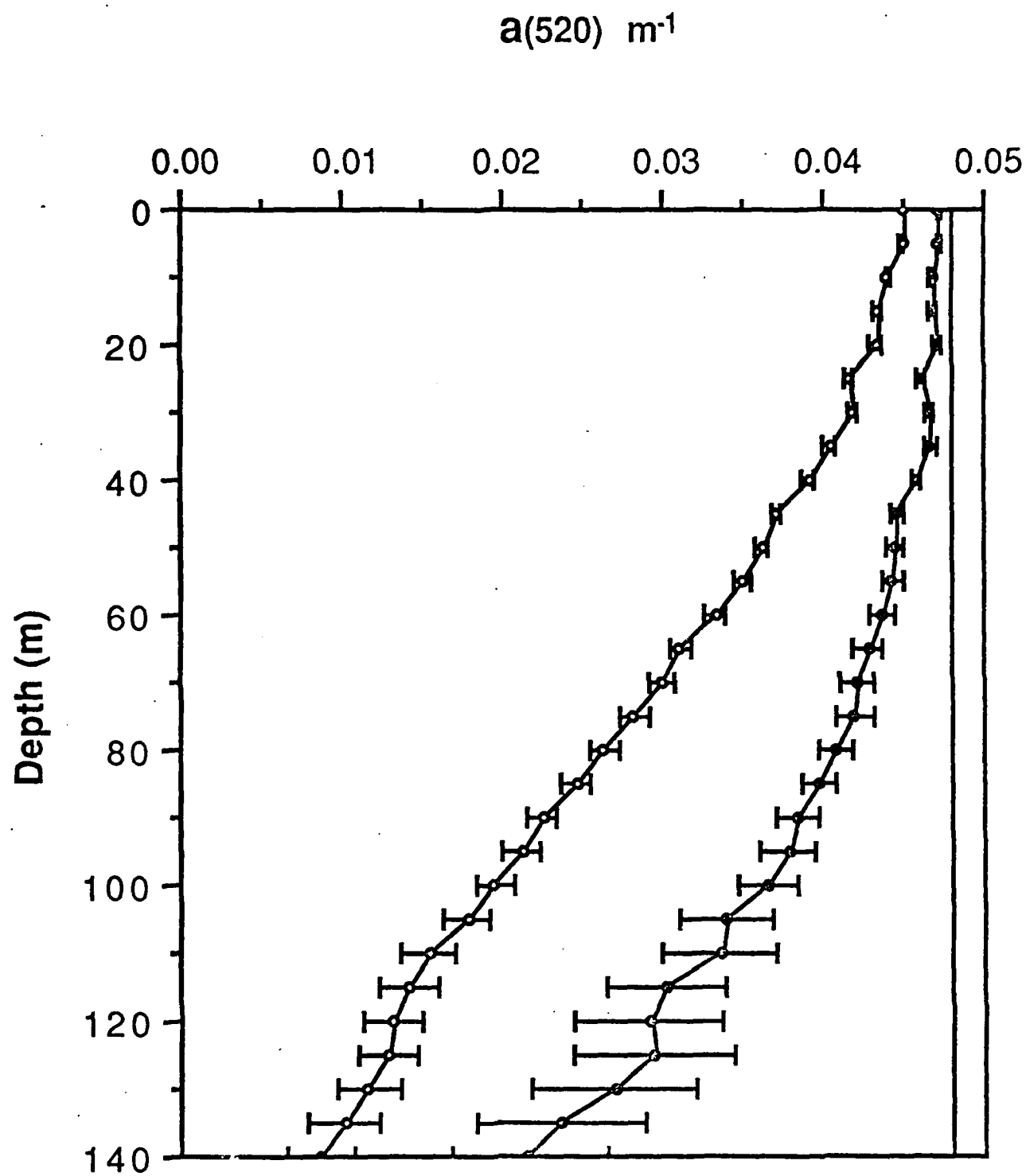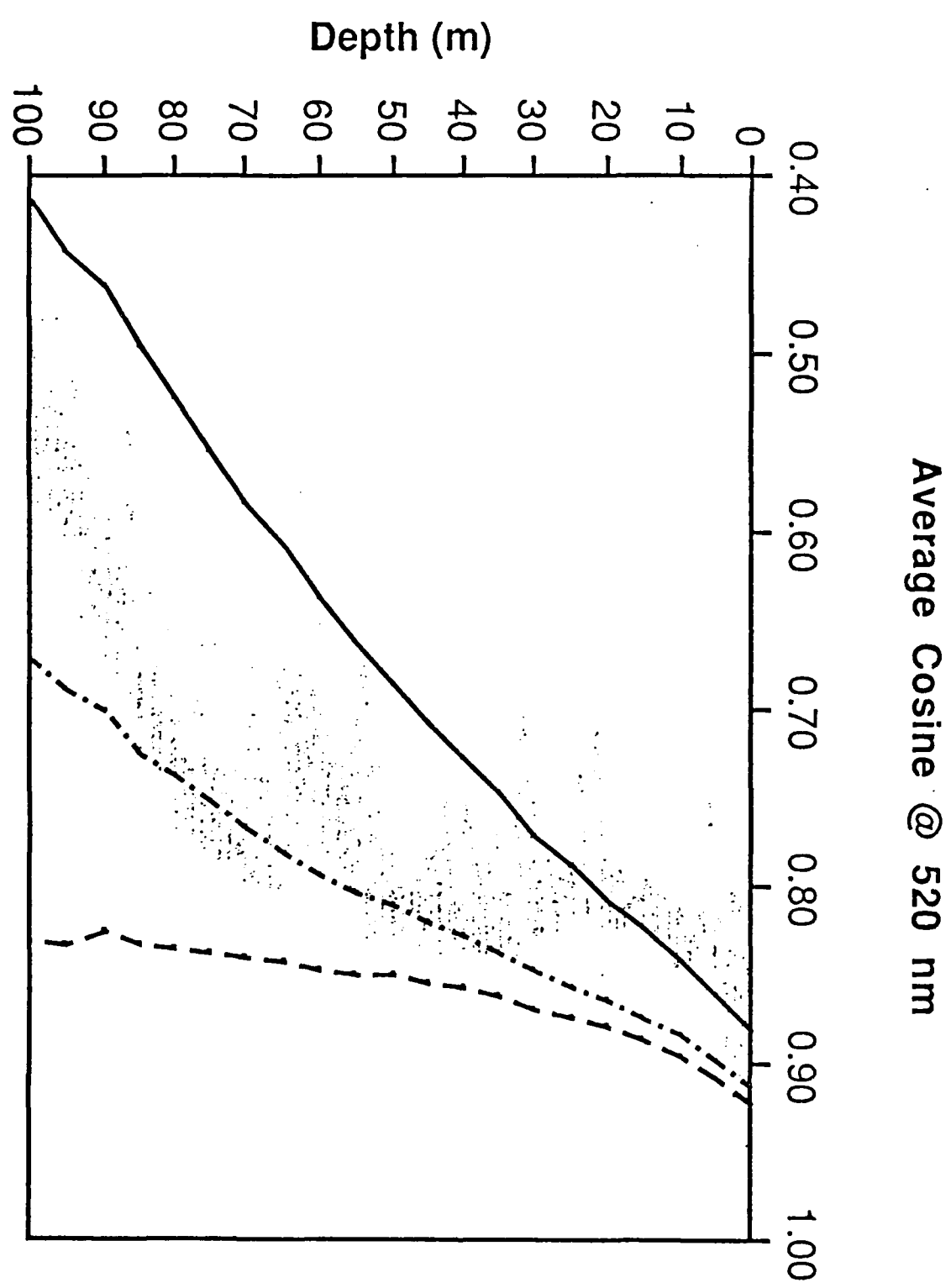
Fig. 9

Depth (m)

Average Cosine @ 520 nm

INITIAL DISTRIBUTION LIST

1. Office of Naval Research   2
   800 North Quincy Street
   Arlington, VA 22217-5000
   Dr. Ann Bucklin, Code 1123B
   Dr. Richard Spinrad, Code 1123OP

2. Naval Research Laboratory   1
   Washington, DC 20375
   Director, Code 2627

3. Defense Technical Information Center   12
   Bldg. 5, Cameron Station
   Alexandria, VA 22314

4. Naval Ocean Research and Development Activity   1
   Natonal Space Technology Laboratories, MS 39529-5004
   Dr. Rudolph Hollman, Code 331

END

DATE

FILMED

DTIC

9-88